Slow excitation supports propagation of slow pulses in networks of excitatory and inhibitory populations

David Golomb
Department of Physiology and Zlotowski Center for Neuroscience, Faculty of Health Sciences, Ben Gurion University of the Negev, Be'er-Sheva 84105, Israel

G. Bard Ermentrout
Department of Mathematics, University of Pittsburgh, Pittsburgh, Pennsylvania 15260
(Received 4 December 2001; published 25 June 2002)

We study the propagation of traveling solitary pulses in one-dimensional networks of excitatory and inhibitory neurons. Each neuron is represented by the integrate-and-fire model, and is allowed to fire only one spike. Two types of propagating pulses are observed. During fast pulses, inhibitory neurons fire a short time before or after the excitatory neurons. During slow pulses, inhibitory cells fire well before neighboring excitatory cells, and potentials of excitatory cells become negative and then positive before they fire. There is a bistable parameter regime in which both fast and slow pulses can propagate. Fast pulses can propagate at low levels of inhibition, are affected by fast excitation but are almost unaffected by slow excitation, and are easily elicited by stimulating groups of neurons. In contrast, slow pulses can propagate at intermediate levels of inhibition, and are difficult to evoke. They can propagate without slow excitation, but slow excitation makes their propagation substantially more robust. Fast pulses can propagate in a wider parameter regime if inhibition decays slowly with time, whereas slow pulses can propagate in a wider parameter regime if the passive time constant of inhibitory cells is large. Strong inhibitory-to-inhibitory conductance eliminates the slow pulses and converts the fast traveling pulses into irregular pulses, in which the inhibitory neurons segregate into two groups that have different firing delays with respect to their neighboring excitatory cells. In general, the velocity of the fast pulse increases with the axonal conductance velocity c, but there are cases in which it decreases with c. We suggest that the fast and slow pulses observed in our model correspond to the fast and slow propagating activity observed in experiments on neocortical slices.

DOI: 10.1103/PhysRevE.65.061911 PACS number(s): 87.19.La, 87.10.+e, 05.45.−a

I. INTRODUCTION

Epilepticlike discharges can propagate in cortical slices when the strength of inhibition is reduced by only 10–20 % [1,2], but they cannot propagate in healthy cortical slices under physiological conditions when inhibition is intact. Inhibition shapes the form of these pulses, and reduces their velocity [1]. Recent experiments in rodents [3,4] and ferrets [5] revealed a different type of propagating pulse in cortical tissue when inhibition is intact or partially reduced. This activity is nonepileptic, with firing rate of individual neurons that is typically low (<10 Hz). The generation and termination of this propagating state may account for the generation of a subset of cortical rhythm during sleep. In intact ferret slices, the propagating velocity is slow, about 1.1 cm/s [5]. When inhibition is blocked, the activity becomes epilepticlike and the velocity becomes fast, about 9 cm/s. The propagation of slow pulses depends on the existence of slow *N*-methyl-D-aspartate (NMDA-mediated) excitation. When this excitation is blocked, the slow pulse often, but not always, cannot propagate [5]. In contrast, blocking the slow excitation does not prevent the propagation of the fast pulses [6]. Blocking the fast α-amino-3-hydroxy-5-methyl-4-isoxazolepropionic acid (AMPA-mediated) excitation prevents the appearance of both fast and slow pulses [5,6].

A large amount of theoretical work has been devoted to networks composed of excitatory neurons only with spatially decaying connectivity [6–10]. We studied networks of excitatory and inhibitory populations with fast synapses in an abstract form [11] and in a Letter [12]. We found that fast pulses can propagate in those systems either without or with small levels of inhibition. In addition, we discovered that slow pulses can propagate at intermediate levels of inhibition, but only in a restricted parameter regime. There is also a bistable regime in which the two pulse types can propagate. The existence of slow and fast pulses in the model, as well as in experiments, raises the following theoretical questions:

(1) How is propagation mediated by excitatory synapses with various kinetics? Can slow pulses propagate in a more robust manner if the system includes slow excitatory synapses?

(2) What are the types of transition from fast to slow propagation as inhibition is enhanced?

(3) How is the initiation of the pulses affected by initial conditions?

(4) How does the appearance of the two pulse types depend on the strength and the connectivity ranges of the various synaptic coupling conductances?

(5) How do time constants of inhibitory cells and synapses affect propagation?

(6) What are the effects of finite axonal velocity?

To answer these questions, we further analyze our simple model of a network composed of excitatory and inhibitory neurons. The single cell is represented by a simplified version of the integrate-and-fire neuronal model, in which a neuron is allowed to fire only one spike, and then it is silent

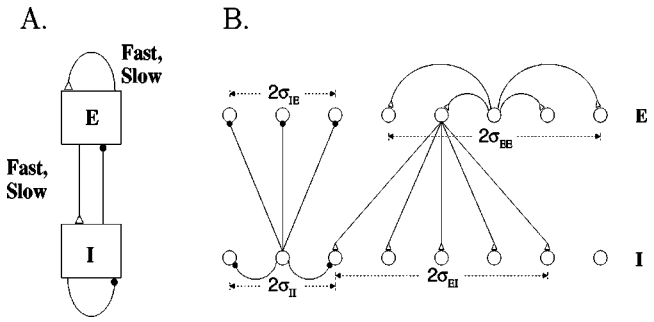

FIG. 1. Schematic diagram of the model architecture. (a) Neuronal populations and synaptic types. (b) The one-dimensional architecture of the network.

forever. This model, which is exact in the limit of a very long refractory period or very strong synaptic depression, is amenable to analytical treatment. The velocity of traveling pulses in this model, their stability, and the delay between the firing times of neighboring excitatory and inhibitory cells during the pulse, are calculated analytically. In particular, we investigate the role of the slow excitation in supporting the propagation of the slow pulse.

The paper is organized as follows. The model is presented in Sec. II. The mathematical analysis of existence and stability of traveling pulse solutions and the calculation of velocity and lag between excitatory and inhibitory cells during the pulses are described in Sec. III. Based on this analysis, we investigate the properties of fast and slow pulses, neglecting axonal conduction velocity in Sec. IV. Effects of finite axonal velocity are described in Sec. V. The results and conclusions are discussed in Sec. VI.

II. THE MODEL

A. Model definition

We consider a one-dimensional network of excitatory (E) and inhibitory (I) neurons [Fig. 1(a)]. A neuron is described by its membrane potential $V_\alpha(x,t)$, $\alpha=E,I$, and its dynamics is governed by the integrate-and-fire scheme in the excitable regime [9]

$$\frac{\partial V_\alpha(x,t)}{\partial t}=-\frac{V_\alpha(x,t)}{\tau_{0\alpha}}+I_{\mathrm{syn},E\alpha}(x,t)-I_{\mathrm{syn},I\alpha}(x,t). \quad (1)$$

Here, $\tau_{0\alpha}$ is the passive membrane time constant of the neuron, and $I_{\mathrm{syn},E\alpha}$ (resp. $I_{\mathrm{syn},I\alpha}$) is the total synaptic current contributed by the excitatory (resp. inhibitory) population.

When the membrane potential of a neuron V reaches a threshold $V_{T\alpha}$, the neuron fires a spike, after which it becomes silent forever. This ''single-spike'' model is exact in the limit of very long refractory period or very strong synaptic depression [13]. In the following, we denote by $T_\alpha(x)$ the time at which a neuron located at x fires. A presynaptic spike induces a postsynaptic current that is proportional to the function $\alpha_{\beta\alpha}(t)$, where

$$\alpha_{\beta\alpha}(t)=\begin{cases}\dfrac{1}{\tau_{s\beta\alpha}}\exp(-t/\tau_{s\beta\alpha}) & t\geqslant 0,\\ 0 & \text{otherwise.}\end{cases} \quad (2)$$

For the excitatory coupling, we consider two types of synaptic current: a fast (f) current and and a slow (s) current, corresponding to the contribution of AMPA and NMDA synaptic receptors in a biological network, respectively. The function $\alpha_{E\alpha}(t)$ and the decay time $\tau_{sE\alpha}$ have a superscript $\gamma=\{f,s\}$ denoting whether the decay of the excitatory current is fast or slow.

The network architecture is shown in Fig. 1(b). The contributions to the synaptic current from the excitatory and inhibitory populations are

$$I_{\mathrm{syn},E\alpha}(x,t)=\sum_{\gamma=f,s} g_{E\alpha}^{\gamma}\int_{-\infty}^{\infty}dx'\, w_{E\alpha}(x-x') \times\alpha_{E\alpha}^{\gamma}(t-T_E(x')), \quad (3)$$

$$I_{\mathrm{syn},I\alpha}(x,t)=g_{I\alpha}\int_{-\infty}^{\infty}dx' w_{I\alpha}(x-x')\,\alpha_{I\alpha}(t-T_I(x')), \quad (4)$$

where $g_{\beta\alpha}$ is the synaptic coupling strength from the β population to the α population. The spatial dependence of the synaptic strength on distance (''synaptic footprint shape'') is given by

$$w_{\beta\alpha}(x)=\frac{1}{2\sigma_{\beta\alpha}}\exp(-|x|/\sigma_{\beta\alpha}). \quad (5)$$

The spatial variable x is dimensionless and represents the distance in terms of the excitatory footprint σ_{EE} that is set to 1. As a result, the velocity ν has units of ms^{-1}.

B. Reference parameter set

In the following, we study the model in its general form. Numerical examples, however, are shown for a particular set of parameters, called the ''reference parameter set,'' with $\tau_{0E}=\tau_{0I}=30$ ms, $\tau_{sEE}^{f}=\tau_{sEI}^{f}=2.5$ ms, $\tau_{sEE}^{s}=\tau_{sEI}^{s}=50$ ms, $\tau_{sIE}=\tau_{sII}=8$ ms, $g_{EE}^{f}=12$, $g_{EE}^{s}=10$, $\sigma_{EE}=1$, $g_{IE}=5.2$, $\sigma_{IE}=0.5$, $g_{EI}^{f}=30$, $g_{EI}^{s}=0$, $\sigma_{EI}=1$, $g_{II}=2$, $\sigma_{II}=0.5$, $V_{TE}=V_{TI}=1$. These parameters are used unless stated otherwise. Since the slow E-to-I excitation g_{EI}^{s} does not have a strong effect on the network dynamics, we consider it to be zero.

III. ANALYSIS OF TRAVELING PULSE SOLUTIONS

A. Volterra representation

In order to analyze the dynamics, we define the Green's function $G_{\beta\alpha}(t)$ for $t>0$ as

$$\frac{dG_{\beta\alpha}}{dt}=-\frac{G_{\beta\alpha}}{\tau_{0\alpha}}+\alpha_{\beta\alpha}(t) \quad (6)$$

and $G_{\beta\alpha}=0$ for $t<0$. The functions $G_{E\alpha}$ have also a superscript γ. For $t>0$, we obtain

$$G_{\beta\alpha}(t)=\frac{\tau_{0\alpha}}{\tau_{0\alpha}-\tau_{s\beta\alpha}}[\exp(-t/\tau_{0\alpha})-\exp(-t/\tau_{s\beta\alpha})]. \tag{7}$$

The integrated form of Eqs. (1), (3), (4) is given by the two Volterra equations for $\alpha=E,I$:

$$V_{T\alpha}=\sum_{\gamma=f,s} g^{\gamma}_{E\alpha}\int_{-\infty}^{\infty} dx' w_{E\alpha}(x')G^{\gamma}_{E\alpha}[T_{\alpha}(x)-T_E(x-x')] - g_{I\alpha}\int_{-\infty}^{\infty} dx' w_{I\alpha}(x')G_{I\alpha}[T_{\alpha}(x)-T_I(x-x')]. \tag{8}$$

In addition, the neuronal voltage should be below threshold before spiking (''causality criterion''),

$$V_{\alpha}(x,t)<V_{T\alpha} \quad \text{for all} \quad t<T_{\alpha}(x), \quad \alpha=E,I. \tag{9}$$

A necessary, but not sufficient, condition for this is

$$\left.\frac{dV_{\alpha}[x,t]}{dt}\right|_{t=T_{\alpha}(x)}>0, \quad \alpha=E,I. \tag{10}$$

B. Existence of traveling pulses

We consider a traveling pulse solution with velocity ν. Without loss of generality, we assume that $\nu>0$. The firing time of an inhibitory cell lags after the firing time of an excitatory cell at the same position by ζ,

$$T_E(x)=\frac{x}{\nu}, \quad T_I(x)=\frac{x}{\nu}+\zeta. \tag{11}$$

Negative ζ means that an I cell fires before a neighboring E cell. Substituting Eq. (11) into Eq. (8) yields

$$V_{T\alpha}=B^{f}_{E\alpha}+B^{s}_{E\alpha}-B_{I\alpha}, \tag{12}$$

where

$$B^{\gamma}_{\beta\alpha}=g^{\gamma}_{\beta\alpha}\int_0^{\infty} dx\, w_{\beta\alpha}(x+\zeta\,\nu\, s_{\beta\alpha})G^{\gamma}_{\beta\alpha}\left(\frac{x}{\nu}\right). \tag{13}$$

We define $s_{\beta\alpha}=(s_{\alpha}-s_{\beta})/2$, where $s_E=1$ and $s_I=-1$. Substituting the expressions for $G_{\beta\alpha}$ and $w_{\beta\alpha}$ in Eqs. (12), (13), we obtain two algebraic equations for ν and ζ, for negative ζ,

$$V_{TE}=\frac{\tau_{0E}\,\nu\,\sigma_{EE}}{2(\nu\,\tau_{0E}+\sigma_{EE})}\sum_{\gamma} g^{\gamma}_{EE}\frac{1}{(\nu\,\tau^{\gamma}_{sEE}+\sigma_{EE})} - g_{IE}\frac{\tau_{0E}\nu}{(\tau_{0E}-\tau_{sIE})}\left[\frac{\tau^2_{0E}\,\nu}{\nu^2\,\tau^2_{0E}-\sigma^2_{IE}}\exp\left(\frac{\zeta}{\tau_{0E}}\right) - \frac{\tau^2_{sIE}\,\nu}{\nu^2\,\tau^2_{sIE}-\sigma^2_{IE}}\exp\left(\frac{\zeta}{\tau_{sIE}}\right) + \frac{(\tau_{0E}-\tau_{sIE})\sigma_{IE}}{2(\nu\,\tau_{0E}-\sigma_{IE})(\nu\,\tau_{sIE}-\sigma_{IE})}\exp\left(\frac{\zeta\nu}{\sigma_{IE}}\right)\right], \tag{14}$$

$$V_{TI}=\frac{\tau_{0I}\,\nu\,\sigma_{EI}}{2(\nu\,\tau_{0I}+\sigma_{EI})}\exp\left(\frac{\zeta\nu}{\sigma_{EI}}\right)\sum_{\gamma} g^{\gamma}_{EI}\frac{1}{(\nu\,\tau^{\gamma}_{sEI}+\sigma_{EI})} - g_{II}\frac{\tau_{0I}\,\nu\,\sigma_{II}}{2(\nu\,\tau_{0I}+\sigma_{II})(\nu\,\tau_{sII}+\sigma_{II})}. \tag{15}$$

Similarly, for positive ζ, we obtain the following two algebraic equations for ν and ζ:

$$V_{TE}=\frac{\tau_{0E}\,\nu\,\sigma_{EE}}{2(\nu\,\tau_{0E}+\sigma_{EE})}\sum_{\gamma} g^{\gamma}_{EE}\frac{1}{(\nu\,\tau^{\gamma}_{sEE}+\sigma_{EE})} - g_{IE}\frac{\tau_{0E}\,\nu\,\sigma_{IE}}{2(\nu\,\tau_{0E}+\sigma_{IE})(\nu\tau_{sIE}+\sigma_{IE})}\exp\left(\frac{-\zeta\nu}{\sigma_{IE}}\right), \tag{16}$$

$$V_{TI}=\sum_{\gamma} g^{\gamma}_{EI}\frac{\tau_{0I}\,\nu}{(\tau_{0I}-\tau^{\gamma}_{sEI})}\left[\frac{\tau^2_{0I}\,\nu}{\nu^2\,\tau^2_{0I}-\sigma^2_{EI}}\exp\left(\frac{-\zeta}{\tau_{0I}}\right) - \frac{(\tau^{\gamma}_{sEI})^2\,\nu}{\nu^2\,(\tau^{\gamma}_{sEI})^2-\sigma^2_{EI}}\exp\left(\frac{-\zeta}{\tau^{\gamma}_{sEI}}\right) + \frac{(\tau_{0I}-\tau^{\gamma}_{sEI})\sigma_{EI}}{2(\nu\,\tau_{0I}-\sigma_{EI})(\nu\,\tau^{\gamma}_{sEI}-\sigma_{EI})}\exp\left(\frac{-\zeta\nu}{\sigma_{EI}}\right)\right] - g_{II}\frac{\tau_{0I}\,\nu\,\sigma_{II}}{2(\nu\,\tau_{0I}+\sigma_{II})(\nu\,\tau_{sII}+\sigma_{II})}. \tag{17}$$

Propagating pulses exist only if Eqs. (14), (15) have at least one solution ν with $\zeta<0$, or if Eqs. (16), (17) have at least one solution ν with $\zeta>0$.

C. Stability of traveling pulses

Stability of the continuous pulses is calculated by following the growth rate of a small perturbation

$$T_E(x)=x/\nu+\theta_E(x), \tag{18}$$

$$T_I(x)=x/\nu+\zeta+\theta_I(x). \tag{19}$$

Substituting these perturbations in Eq. (8), and keeping only the first-order terms in θ_E, θ_I, we obtain two equations for $\alpha=E,I$,

$$0=\sum_{\gamma=f,s} g^{\gamma}_{E\alpha}\int_{\zeta\,\nu\,s_{E\alpha}}^{\infty} dx' w_{E\alpha}(x')G'^{\gamma}_{E\alpha}\left(\frac{x'}{\nu}-\zeta\,S_{E\alpha}\right) \times[\theta_{\alpha}(x)-\theta_E(x-x')]-g_{I\alpha}\int_{\zeta\,\nu\,s_{I\alpha}}^{\infty} dx' w_{I\alpha}(x') \times G'_{I\alpha}\left(\frac{x'}{\nu}-\zeta\,S_{I\alpha}\right)[\theta_{\alpha}(x)-\theta_I(x-x')], \tag{20}$$

where

$$G'(t)=dG(t)/dt. \tag{21}$$

Assuming that the perturbations evolve as $\theta_E(x)=\theta_{E0}\exp(\lambda x)$ and $\theta_I(x)=\theta_{I0}\exp(\lambda x)$, yields the matrix equation

$$\sum_{\beta=E,I} A_{\beta\alpha}(\lambda)\,\theta_{\beta 0}=0, \tag{22}$$

where

$$A_{EE}(\lambda)=\sum_{\gamma} g_{EE}^{\gamma}\int_0^{\infty} dx\, w_{EE}(x)G'^{\gamma}_{EE}\left(\frac{x}{\nu}\right)(1-e^{-\lambda x}) - g_{IE}\int_{\zeta\nu}^{\infty} dx\, w_{IE}(x)G'_{IE}\left(\frac{x}{\nu}-\zeta\right), \tag{23}$$

$$A_{IE}(\lambda)=g_{IE}\int_{\zeta\nu}^{\infty} dx\, w_{IE}(x)G'_{IE}\left(\frac{x}{\nu}-\zeta\right)e^{-\lambda x}, \tag{24}$$

$$A_{EI}(\lambda)=-\sum_{\gamma} g_{EI}^{\gamma}\int_{-\zeta\nu}^{\infty} dx\, w_{EI}(x)G'^{\gamma}_{EI}\left(\frac{x}{\nu}+\zeta\right)e^{-\lambda x}, \tag{25}$$

$$A_{II}(\lambda)=\sum_{\gamma} g_{EI}^{\gamma}\int_{-\zeta\nu}^{\infty} dx\, w_{EI}(x)G'^{\gamma}_{EI}\left(\frac{x}{\nu}+\zeta\right) - g_{II}\int_0^{\infty} dx\, w_{II}(x)G'_{II}\left(\frac{x}{\nu}\right)(1-e^{-\lambda x}). \tag{26}$$

Equation (22) has nontrivial solutions if

$$\det[A(\lambda)]=0. \tag{27}$$

The value $\lambda=0$ is always a solution of the characteristic equation (27) because of the translation invariance. Apart from this marginal stability, the traveling pulse is stable if all the other solutions of this equation have negative real parts. The values of $A_{\beta\alpha}(\lambda)$ for Eqs. (2), (5) are given in Appendix A.

A pulse can lose stability at a saddle-node bifurcation (SNB), where the $\lambda=0$ solution to Eq. (27) is a double zero, namely,

$$d\{\det[A(\lambda)]\}/d\lambda|_{\lambda=0}=0. \tag{28}$$

Alternatively, a pulse can lose stability at a Hopf bifurcation (HB), where Eq. (27) has two imaginary solutions with $\lambda=\pm i\omega$.

D. Activity of *I* cells

We have studied the existence and stability of the traveling solution, Eq. (11), under the assumption that both *E* and *I* cells participate in the firing. With small g_{EI}^{γ}, $\gamma=s,f$, however, there may be a situation in which only the *E* cells fire, whereas the *I* cells are quiescent. In order to determine whether for particular g_{EI}^{γ} the *I* cells are excited, we realize

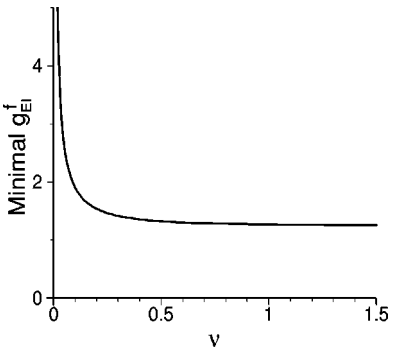

FIG. 2. The minimal g_{EI}^f for which the *I* cells are recruited to the pulse as a function of ν. The reference parameter set is used (except for g_{EI}^f); in particular, $g_{EI}^s=0$. As $\nu\to\infty$, the minimal g_{EI}^f value, 1.253, is given by Eq. (33).

that if the *I* cells are quiescent, ν is determined solely from the interactions between the *E* cells [Eq. (14)],

$$V_{TE}=\frac{\tau_{0E}\nu\sigma_{EE}}{2(\nu\tau_{0E}+\sigma_{EE})}\sum_{\gamma=f,s} g_{EE}^{\gamma}\frac{1}{(\nu\tau_{sEE}^{\gamma}+\sigma_{EE})}. \tag{29}$$

The *I* cells do not fire if their voltage is below their threshold, V_{TI} for all $t>0$. Without loss of generality, we consider a traveling excitatory pulse $T_E(x)=x/\nu$ affecting an inhibitory neuron located at $x=0$. The voltage of this *I* neuron is given by Eqs. (1), (3), (4), and (6),

$$V_I(0,t)=\sum_{\gamma=f,s} g_{EI}^{\gamma}\int_{-t\nu}^{\infty} dx w_{EI}(x)G_{EI}^{\gamma}\left(t+\frac{x}{\nu}\right). \tag{30}$$

For $t<0$, V_I is

$$V_I(0,t)=\frac{\tau_{0I}\nu\sigma_{EI}}{2(\nu\tau_{0I}+\sigma_{EI})}\exp\left(\frac{t\nu}{\sigma_{EI}}\right)\sum_{\gamma=f,s} g_{EI}^{\gamma}\frac{1}{(\nu\tau_{sEI}^{\gamma}+\sigma_{EI})} \tag{31}$$

and for $t>0$, it is

$$V_I(0,t)=\nu\tau_{0I}\sum_{\gamma=f,s} g_{EI}^{\gamma}\left[\frac{-\nu\tau_{0I}^2\exp(-t/\tau_{0I})}{(\tau_{0I}-\tau_{sEI}^{\gamma})(\sigma_{EI}+\nu\tau_{0I})(\sigma_{EI}-\nu\tau_{0I})} + \frac{\nu(\tau_{sEI}^{\gamma})^2\exp(-t/\tau_{sEI}^{\gamma})}{(\tau_{0I}-\tau_{sEI}^{\gamma})(\sigma_{EI}+\nu\tau_{sEI}^{\gamma})(\sigma_{EI}-\nu\tau_{sEI}^{\gamma})} + \frac{\sigma_{EI}\exp(-\nu t/\sigma_{EI})}{2(\sigma_{EI}-\nu\tau_{0I})(\sigma_{EI}-\nu\tau_{sEI}^{\gamma})}\right]. \tag{32}$$

The *I* cells are recruited by the traveling pulse if there is a value of t such that $V_I(0,t)=V_{TI}$. The dependence of the minimal g_{EI}^f for which the *I* cells are recruited on ν is shown in Fig. 2 for the reference parameter set (in which $g_{EI}^s=0$). For $\nu\to\infty$ and $g_{EI}^s=0$, the minimal g_{EI}^f is

$$(g_{EI}^f)_{\text{minimal}}/V_{TI}=\left(\frac{\tau_{sEI}^f}{\tau_{0I}}\right)^{\tau_{sEI}^f/(\tau_{sEI}^f-\tau_{0I})}. \tag{33}$$

As seen in Fig. 2, the values of $(g_{EI}^f)_{\text{minimal}}$ for ν of order 1 ms^{-1} are close to that asymptotic value.

E. Voltage profile

For a traveling pulse, the voltage profile of the E and I neurons that have not fired is determined by the voltage profile of the neurons at time $t=0$,

$$V_\alpha(x,t)=V_\alpha(x-\nu t,0), \quad \alpha=E,I. \tag{34}$$

We calculate $V_E(x-\nu t,0)$ in the domain $0\leqslant x\leqslant\infty$ and $V_I(x-\nu t,0)$ in the domain $-\zeta\nu\leqslant x\leqslant\infty$ using Eqs. (1), (3), (4), and (6) and obtain

$$V_\alpha(x,0)=\sum_{\gamma=f,s} g_{E\alpha}^\gamma\int_0^\infty dx' w_{E\alpha}(x+x')G_{E\alpha}^\gamma\left(\frac{x'}{\nu}\right) - g_{I\alpha}\int_{\zeta\nu}^\infty dx' w_{I\alpha}(x+x')G_{I\alpha}\left(\frac{x'}{\nu}-\zeta\right). \tag{35}$$

The values of $V_\alpha(x,0)$ for $\zeta<0$ are given in Appendix B. Numerical techniques used throughout this article are described in Appendix C.

IV. PROPAGATION OF PULSES IN NETWORKS WITH INHIBITION AND SLOW EXCITATION

The main goal of this paper is to study the effects of inhibition on pulse propagation. Therefore, we emphasize the effects of the parameter g_{IE} and study how it modifies the system dynamics under various conditions. Effects of other parameters are also studied.

A. The dependence of the existence and stability of slow and fast pulses on inhibition and slow excitation

The dependence of ν (upper and middle panels) and ζ (lower panels) on g_{IE} is shown in Figs. 3(a)–3(c) for the reference parameter set, three values of g_{EI}^f, and two values of g_{EE}^s: 0 (thin lines) and 10 (thick lines). We first describe the situation for $g_{EE}^s=0$. At low g_{EI}^f values, there is only one stable branch of ''fast'' pulses, which terminates at a SNB. At intermediate g_{EI}^f values, bistability exists, and at intermediate g_{IE} values both the fast pulse and the slow pulse can propagate. The g_{IE} regime in which bistability exists is pretty restricted, because the slow pulse is terminated by a HB. At large g_{EI}^f values, there is a crossover between fast pulses and a slow pulses as g_{IE} increases. The slow pulse is still destabilized by an HB at a certain g_{IE} value. Whereas our theory cannot determine what happens for g_{IE} larger than its value at the HB, extensive numerical simulations indicate that no pulse can propagate in that regime. This situation is different from the case of excitatory networks with delay [10], where the HB leads to the propagation of discontinuous, ''lurching'' pulses. Increasing g_{EE}^s to 10 modifies the ν-g_{IE} curve in two aspects. First, the branch in the bifurcation diagram corresponding to the slow pulse extends for wider g_{IE} region. Second, there is no HB. As a result, the slow E-to-E excitation increases the regime where stable slow pulses can propagate. For all the g_{EE}^s and g_{EI}^f values, the time difference $|\zeta|$ increases as ν decreases, and therefore the time lead of the I cell is larger for the slow pulse than for the fast pulse.

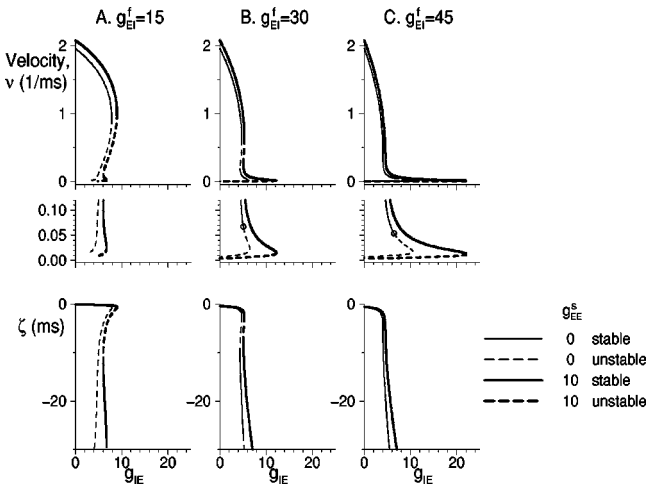

FIG. 3. The velocity ν of propagating pulses (upper and middle panels), and the difference ζ between the firing times of inhibitory and excitatory cells at the same position (lower panels), as functions of inhibitory-to-excitatory synaptic strength g_{IE} for the reference parameter set and three values of the excitatory-to-inhibitory synaptic strength g_{EI}^f: (a) $g_{EI}^f=15$. (b) $g_{EI}^f=30$. (c) $g_{EI}^f=45$. Thick lines represent pulses with $g_{EE}^s=10$, and thin lines represent pulses with $g_{EE}^s=0$. Solid lines represent stable pulses and dashed lines represent unstable pulses. In the middle panels, which are expansions of the upper panels, Hopf bifurcations are denoted by open circles. Bistability of fast and slow pulses is observed for moderate values of g_{EI}^f and g_{IE}.

For all the parameter regimes we have examined, E cells fire before or slightly after the I cells during the fast pulse, and the values of ζ are small positive or negative values, of order 1 ms. In contrast, during the propagation of the slow pulse, E cells fire well after the I cells, and ζ is negative, on the order of a few tens of ms. The slow pulse can therefore be viewed as a front of I cells' spikes pushed from behind by the E cells' spikes; because each E cell receives strong inhibition from neurons in front of it, the pulse propagates slowly.

In addition to the branches of solution shown in Fig. 3, two other unstable branches may appear. In one of them, excitatory cells lead in firing. These branches do not usually affect the system dynamics, except for within specific parameter regimes that will be described below.

The voltage profile of neurons that have not fired yet at time $t=0$ is shown in Fig. 4 for the reference parameter set. With this set of parameters, the fast pulse and the slow pulse coexist. During the fast pulse, the membrane potential of a neuron at a position x decays monotonically with distance from the pulse. During the slow pulse, the potential of the I cells also decays monotonically. However, during the slow pulse, the potential of the E cell first decays rapidly and reaches a negative value. Then, it increases to positive values and then decreases again. Note that a mirror image of the same profile, with the abscissa stretched by a factor of $1/\nu$,

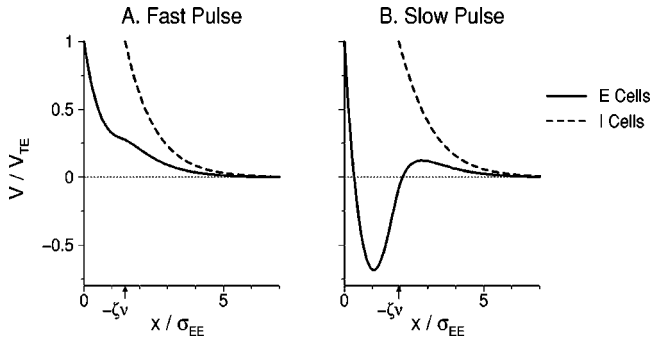

FIG. 4. The potentials V of excitatory neurons (solid line) and inhibitory neurons (dashed line) that have not fired yet at time $t=0$ are plotted as a function of their position. The reference parameter set is used; in particular, $g_{IE}=5.2$ and $g_{EE}^{s}=10$. (a) Potentials during the fast pulse. (b) Potentials during the slow pulse.

describes the temporal behavior of the pulse at a constant position x. This means that during the slow pulse, each excitatory neuron is first excited, but then is affected by strong inhibition and its potential becomes negative. Only when the pulse continues to propagate and the effect of inhibition is diminished, is the neuron again affected by excitation and so can reach threshold and fire.

Plotting the voltage profile as a function of x (Fig. 4) demonstrates a case in which ν and ζ are different for the fast pulse and the slow pulse, but the value of $\nu\zeta$ is similar. Since the footprint ranges in the model are of order 1, the value $|\nu\zeta|$ should be of order 1 or less, otherwise the spikes emitted by neurons from one population do not affect neurons in the other population. Hence, lower ν enables ζ to have larger values, that can be, in principle, negative or positive.

To further demonstrate that g_{EE}^{s} increases the regime of slow-pulse propagation, we present in Fig. 5 two-dimensional bifurcation diagrams in the g_{EI}^{f}-g_{IE} plane, for $g_{EE}^{s}=0$ [Fig. 5(a)] and $g_{EE}^{s}=10$ [Fig. 5(b)]. The fast pulse exists for $g_{IE}\gtrsim 0$ for all g_{EI}^{f} values. Three lines of SNB are plotted. The lower SNB line (dashed), corresponding to the minimal g_{IE} value above which the fast pulse can propagate, is bounded by two codimension-2 cusp bifurcations [14]. The cusp at low g_{EI}^{f}, denoted by the asterisk, produces the slow-pulse branch as a ''ripple'' on an unstable solution [see Fig. 3(a), thick line]. The cusp at high g_{EI}^{f}, denoted by the diamond, connects the slow and the fast branches, and eliminates the unstable branch between them. At higher g_{EI}^{f} values, there is a continuous crossover between the fast branch and the slow branches as g_{EI}^{f} increases. For $g_{EE}^{s}=0$, but not for $g_{EE}^{s}=10$, there is a line of HB representing the maximal g_{IE} above which the slow pulse is unstable. Comparing panels, Figs. 5(a) and 5(b), shows that in Fig. 5(b), the slow-pulse regime, and also the bistable regime (in which the two pulse types can propagate), have larger areas in the two-parameter space for two reasons. First, the slow branch is terminated by a SNB at higher g_{IE} values. Second, the slow branch is not destabilized by a HB if g_{EE}^{s} is large enough.

The contribution of the slow E-to-E excitation to the extension of the regime of stable slow pulses is also shown in

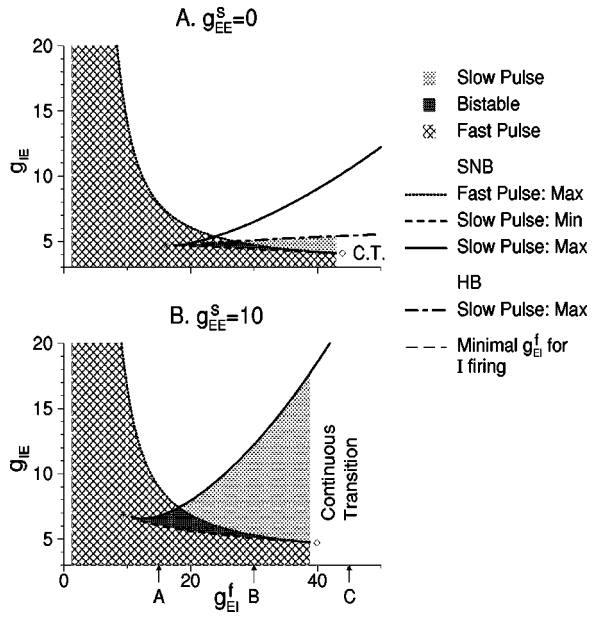

FIG. 5. Regimes of existence and stability of fast and/or slow pulses in the g_{EI}^{f}-g_{IE} plane for the reference parameter set and $g_{EE}^{s}=0$ (a) and $g_{EE}^{s}=10$ (b). Saddle-node bifurcation curves are denoted by thick lines, dotted line, the maximal g_{IE} value of the fast pulse; dashed line, the minimal g_{IE} value of the slow pulse, solid line, the maximal g_{IE} value of the slow pulse. The Hopf bifurcation curve in (a), is denoted by the dot-dashed line. Such a curve does not appear in (b). For g_{EI}^{s} value smaller than the thin long-dashed line, only excitatory cells fire, and inhibitory cells are quiescent. Shadings: dark gray, bistable regime; light gray, regime in which only slow pulses can propagate; mesh of diagonal lines, regime in which only fast pulses can propagate; ''continuous transition'' [or ''C.T.'' in (a)], regime of continuous transition from a fast-pulse behavior for $g_{IE}\gtrsim 0$ to slow-pulse behavior as g_{IE} increases. In all the other white regimes, no pulse can propagate. The cusps of the SNB lines are denoted by an * (left) and by a $\diamond$ (right). The three arrows below the abscissa in (b) represent the three values of g_{EI}^{f} in Fig. 3. Slow excitation increases considerably the parameter regime in which slow pulses can propagate.

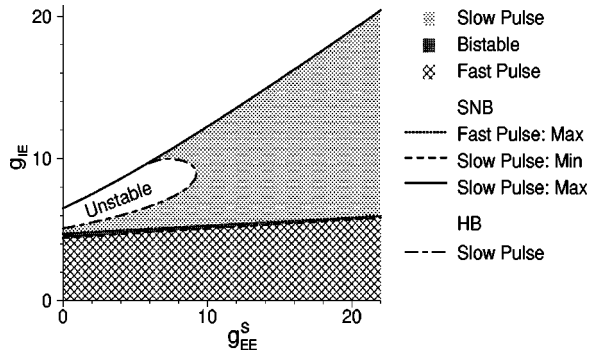

FIG. 6. Regimes of existence and stability of fast and/or slow pulses in the g_{EE}^{s}-g_{IE} plane. The meanings of the lines and the shading are the same as in Fig. 5. In the white regime bounded by the HB line (dot-dashed), the SNB line (solid) and the ordinate, the slow pulse exists, but it is unstable. For g_{IE} values above the solid line, no pulses exist.

the g^s_{EE}-g_{IE} plane in Fig. 6 for the reference parameter set ($g^f_{EI}=30$). The HB destabilizes the slow pulse only for g^s_{EE} values smaller than a certain value (which is $g^s_{EE}=9.24$ here). Note that for a fixed g^s_{EE} value just below that finite value, the slow pulse is stable in two disconnected intervals of g_{IE}, between which it is unstable. The robustness of the slow pulse at larger g^s_{EE} values can be explained by the fact that strong, prolonged *E*-to-*E* excitation helps excitatory neurons to overcome the inhibition imposed on them by the inhibitory neurons that fire first, such that those excitatory neurons can eventually reach threshold and fire.

B. Response to shock initial conditions

Even if, for a particular set of parameters, a pulse exists and is stable, it does not mean that it can be generated using a particular choice of initial conditions. Since the space of initial conditions has, in principle, infinite dimensions, we cannot determine the volume of the basins of attraction for a particular propagating state in that space. Instead, we choose to use one type of initial condition, the ''shock'' initial condition. All the neurons in a region $0<x<2.5$ were excited at $t=0$, and we followed which type of pulse is generated, if at all. The shock initial condition was chosen because it replicates the experimental situation, in which propagating discharges are initiated by a brief spatially localized stimulation [6].

The system's response to shocks is described in Fig. 7 for two values of g^s_{EE}: 0 [Figs. 7(a) and 7(b)] and 10 [Figs. 7(c) and 7(d)]. We compared the responses for two values of ν. We keep all the parameters at their reference values except for g_{IE}, which we tuned in order to obtain the desired value of ν. These g_{IE} and ν values are shown in Fig. 7(e), which is the same as Fig. 3(b) (middle panel). For $g^s_{EE}=0$ and $\nu=0.085$ ms^{-1} [Fig. 7(a)], the slow pulse is the only attracting pulse. A shock stimulus initiates a transient fast pulse that propagates along a considerable distance before it switches to the slow pulse (at about $x=30$). For $\nu=0.072$ ms^{-1} [Fig. 7(b)], the slow pulse is also the only attracting pulse, but a shock stimulus generates a localized activity only that does not propagate. When g^s_{EE} is raised to 10, the same shock stimulus generates a slow pulse for the two values of ν, beyond a small interval of fast propagation [Fig. 7(c)], or after two periods of ''lurching'' activity [Fig. 7(d)].

The effect of the slow excitation can be explained intuitively as following. After a shock stimulus, in order to generate a slow pulse, the firing times of the neurons should reorganize such that the *I* cells fire before the *E* cells at the same position. If there is slow excitation, a cell receives inhibition and excitation due to the fast inhibitory and excitatory synapses, and then, for a prolonged amount of time, slow excitation that enables it to overcome the inhibition and fire. Note that when the fast pulse is the only attractor, shock initial conditions generate it with or without g^s_{EE} for all the cases we examined (not shown).

C. Effects of strength of fast excitation

In the cortex, there is a delicate balance between excitation and inhibition, and deviations from this balance can lead

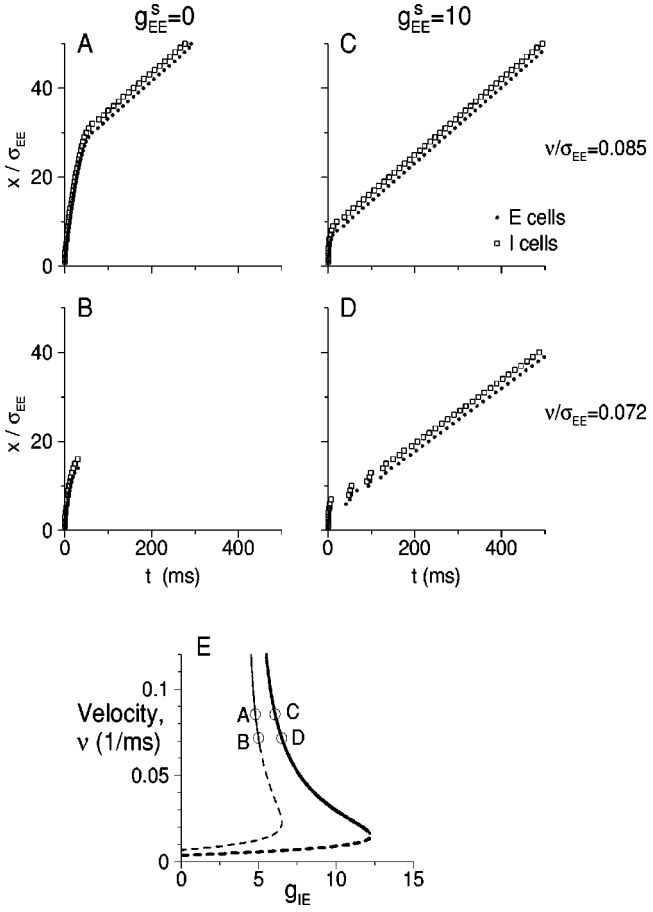

FIG. 7. Network responses to a ''shock'' stimulus are shown in rastergrams [(a)–(d)]. Firing times of excitatory cells are denoted by solid circles, and firing times of inhibitory cells are denoted by open squares. There are $\rho=20$ neurons from each type within each unit length (σ_{EE}), and spikes of only one out of every 20 neurons are plotted. The number of neurons in each population is $N=1000$, and the reference parameter set is used. The network is initiated by an abrupt activation of all the excitatory and inhibitory neurons on the ''left'' ($0<x<2.5$). Simulations are carried out for two values of g^s_{EE} and two values of ν: (a) $g^s_{EE}=0$, $\nu=0.085$ ($g_{IE}=4.8$); (b) $g^s_{EE}=0$, $\nu=0.072$ ($g_{IE}=5$); (c) $g^s_{EE}=10$, $\nu=0.085$ ($g_{IE}=6.08$); (d) $g^s_{EE}=10$ $\nu=0.072$ ($g_{IE}=6.51$). In *E*, the values of g_{IE} and the velocities ν of the slow pulses are shown. The curves, corresponding to slow pulses, are identical to the curve shown in Fig. 3(b) (middle panel). Thick lines represent pulses with $g^s_{EE}=10$, and thin lines represent pulses with $g^s_{EE}=0$. Solid lines represent stable pulses and dashed lines represent unstable pulses. The circles labeled (a)–(d) correspond to the value of g_{IE} and ν in panels (a)–(d). Without slow excitation, it is difficult to evoke slow pulses, even if they exist and are stable.

to the generation of epilepticlike discharges [1], corresponding to the fast pulses in our model. The strength of fast (AMPA-mediated) *E*-to-*E* excitatory conductance may change as a result of learning. For example, Saar *et al.* found indirect evidence for an increase in g^f_{EE} during olfactory learning in rats on the order of tens of percents [15]. Despite this increase, cortical slices do not become more epileptic after learning. A possible explanation to these facts is the *E*-to-*I* excitation and/or the *I*-to-*E* inhibition increase as

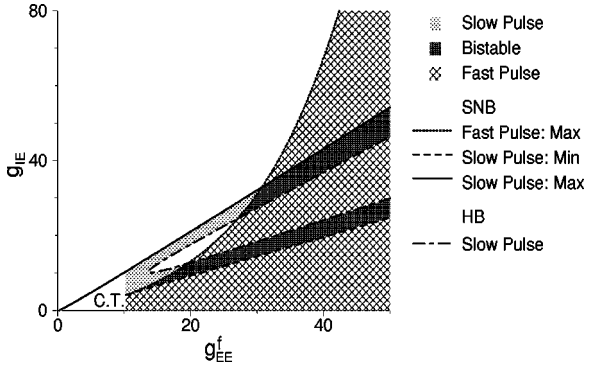

FIG. 8. Regimes of existence and stability of fast and/or slow pulses in the g^f_{EE}-g_{IE} plane. The meanings of the lines and the shading are the same as in Fig. 5. The dotted line, below which the fast pulse can propagate, is convex as a function of g^f_{EE}.

well, and prevent the propagation of the fast pulse. In order to study this hypothesis, we analyze the appearance of propagating pulses in the g^f_{EE}-g_{IE} and g^f_{EE}-g^f_{EI} planes.

The regimes in which the two pulse types can propagate in the g^f_{EE}-g_{IE} plane are shown in Fig. 8. Fast pulses can propagate if g_{IE} is below a certain value $g_{IE,\max}$ that increases with g^f_{EE} (dotted line). The curve of $g_{IE,\max}$ as a function of g^f_{EE} is convex (i.e., it has a positive curvature) and $dg_{IE,\max}/dg^f_{EE}>0$. Therefore, to compensate for an increase of g^f_{EE} and prevent fast-pulse propagation, the enhancement in the level of $g_{IE,\max}$ should itself increase with g^f_{EE}.

The minimal and maximal g_{IE} values for which the slow pulses cease to exist both grow almost linearly with g^f_{EE}, although with different slopes. Interestingly, for a large enough g^f_{EE}, there are two HB points on the slow-pulse branch. The slow pulse is unstable between them and is stable in two separate g_{IE} intervals.

The regimes in which the two pulse types can propagate in the g^f_{EE}-g^f_{EI} plane are shown in Fig. 9(a). Except for a small parameter regime at small g^f_{EE} values, the dependence of the maximal g^f_{EI} value for which fast pulses can propagate (dotted line) is convex and has a positive curvature. This behavior is functionally similar to the dependence of $g_{IE,\max}$ on g^f_{EE} for constant g^f_{EI}. At low g^f_{EI} values, this regime has a ''tail'' that points back toward large g^f_{EE} values.

Slow pulses can propagate if g^f_{EI} is above a certain value $g^f_{EI,\min}$ (dashed line) that first decreases and then increases as a function of g^f_{EE}. The asterisk points to a codimension-2 pitchfork bifurcation (at $g^f_{EE}=11.6$, $g_{IE}=10.6$) of two pairs of SNB solutions. Two more SNB lines, that stem from this pitchfork bifurcation and correspond to the annihilation point of two unstable solutions, are not plotted for simplicity. The pitchfork bifurcation separates two different regimes. To describe them, we should consider another pair of slow-pulse solutions, which are unstable and therefore have been ignored, but here they come to play a role. In order to follow their effect, it is useful to look at Fig. 9(b). For low g^f_{EE} values, such as $g^f_{EE}=8$ (I), a fast-pulse solution is stable at low g^f_{EI}, and is destabilized at a SNB. The resulting unstable

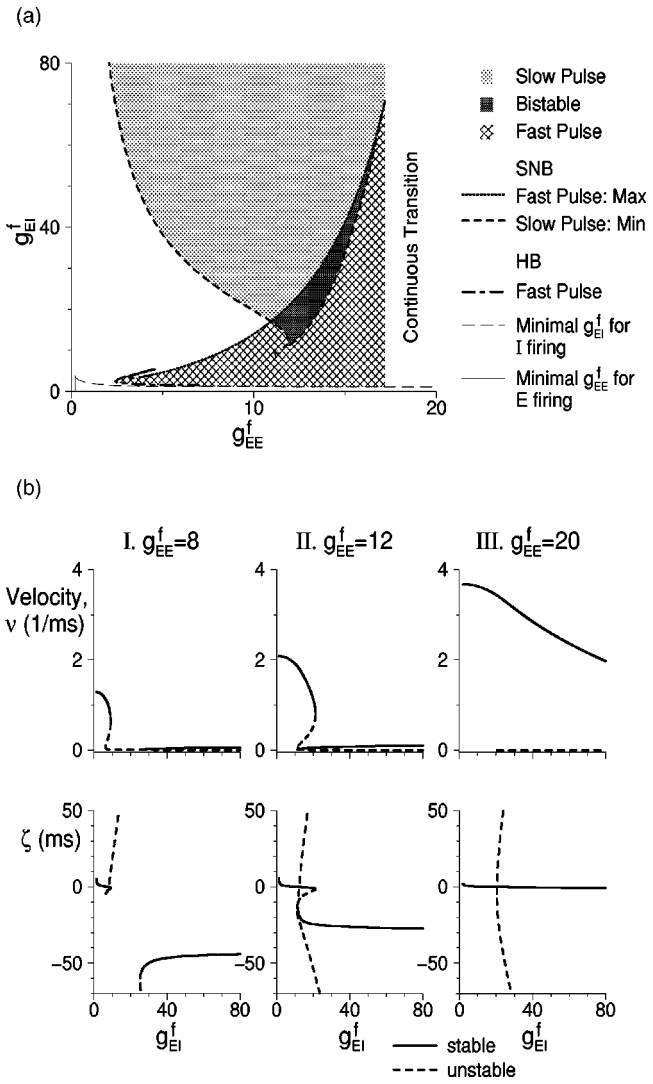

FIG. 9. (a) Regimes of existence and stability of fast and/or slow pulses in the g^f_{EE}-g^f_{EI} plane; $g_{IE}=6.5$. The meanings of the lines and the shading are the same as in Fig. 5. The asterisk points to a codimension-2 pitchfork bifurcation of two pairs of SNB solutions. Two more SNB lines, that stem from this pitchfork bifurcation and correspond to the annihilation point of two unstable solutions, are not plotted for simplicity. In the white regime bounded by the thin long-dashed line, the thin solid line, and the abscissa, only excitatory cells fire as a pulse propagates. The dotted line, below which the fast pulse can propagate, is convex as a function of g^f_{EE}. (b) The velocity ν of propagating pulses (upper panels), and the difference ζ between the firing times of inhibitory and excitatory cells at the same position (lower panels), as functions of g^f_{EI} for the reference parameter set, $g_{IE}=6.5$ and three values of g^f_{EE}: I. $g^f_{EE}=8$. II. $g^f_{EE}=12$. III. $g^f_{EE}=20$. Solid lines represent stable pulses and dashed lines represent unstable pulses.

solution undergoes a second SNB, in which it is connected to an unstable solution with positive ζ values that increase with increasing g^f_{EI}. At larger g^f_{EI} values, a second pair of slow-pulse solutions emerges at a SNB ($g^f_{EI}=25.3$), and the one with larger velocity and smaller $|\zeta|$ is stable. It is easier to view it in the ζ graph (lower panel), because in the ν graph (upper panel) it is hard to distinguish between the slow so-

lutions. At larger g_{EE}^f values, such at $g_{EE}^f=12$ (II), which is slightly larger than the value of g_{EE}^f at the pitchfork, the various branches are differently connected. The fast-pulse solution is destabilized by a SNB as before, but the unstable solution is now connected by a SNB to the stable slow-pulse solution. Two unstable solutions, one with large positive ζ and one with large negative ζ (for large g_{EI}^f) are connected at a SNB, but do not affect the dynamics. At even larger g_{EE}^f values, such as $g_{EE}^f=20$ (III), the fast-pulse solution does not destabilize as g_{EI}^f increases, ν decreases only gradually, and the negative values of ζ have small absolute values (for example, $\zeta=-0.94$ for $g_{EI}^f=80$). This pulse solution does not destabilize even for large g_{EI}^f values as 1000. This means that if g_{EE}^f is large enough, the pulse cannot be prevented by increasing g_{EI}^f alone.

D. Time constants of inhibitory neurons and synapses

When we study the effects of inhibition on pulse propagation, we need to consider the time scales of inhibitory cells and synapses. In our reference parameter set, we assume that the passive time constants of the excitatory and inhibitory neurons are equal. There are indications, however, that some types of inhibitory interneurons have faster passive time constant τ_{0I} in comparison with excitatory neurons [16]. In order to examine the effects of varying τ_{0I} on the pulse propagation, we calculated the regimes in which pulses can propagate in the τ_{0I}-g_{IE} plane, as shown in Fig. 10(a). Large g_{IE} values are needed to prevent the fast pulses from propagating at very small τ_{0I} values. For larger τ_{0I} values, however, the maximal g_{IE} value that allows fast-pulse propagation decreases very weakly with τ_{0I}. The maximal g_{IE} value that allows slow-pulse propagation increases almost linearly with τ_{0I} values if τ_{0I} is not too small.

Varying the τ_{sIE}, the decay time of inhibitory synapses, while keeping the equality $\tau_{sII}=\tau_{sIE}$, causes different effects, as seen in Fig. 10(b). The maximal g_{IE} that is needed for terminating the fast pulse increases linearly with τ_{sIE}. This can be explained by the fact that the synaptic functions $\alpha_{\beta\alpha}(t)$ are normalized such that their integral is 1 [Eq. (2)]. Therefore, the peak of α_{IE} is proportional to $1/\tau_{sIE}$. If τ_{sIE} is increased, g_{IE} should be increased proportionally to keep the level of inhibition just after the spike constant. For fast inhibition (small τ_{sIE}), there is a continuous transition from a fast pulse to a slow pulse as g_{IE} increases. For larger values of τ_{sIE}, the g_{IE} interval for which the slow pulse exists shrinks. Moreover, a Hopf bifurcation destabilizes the slow pulse at middle levels of g_{IE} along this interval. As a result, the slow pulse is stable at moderate τ_{sIE} values only in a small g_{IE} interval; at large τ_{sIE}, it does not exist at all. Interestingly, our numerical calculation of the bifurcation lines shows that the HB line intersects the SNB lines at the cusp (where $\tau_{sIE}=43$), and for τ_{sIE} values just below the cusp it runs just above, but very close to, the lower SNB line. Since the eigenvalues corresponding to the HB remain bounded away from zero as the curve hits the SNB, this point is not a Takens-Bogdonav point (double zero eigenvalue). Rather it is the fold-Hopf bifurcation [17] in which there is simultaneously a pair of imaginary eigenvalues and a zero eigenvalue.

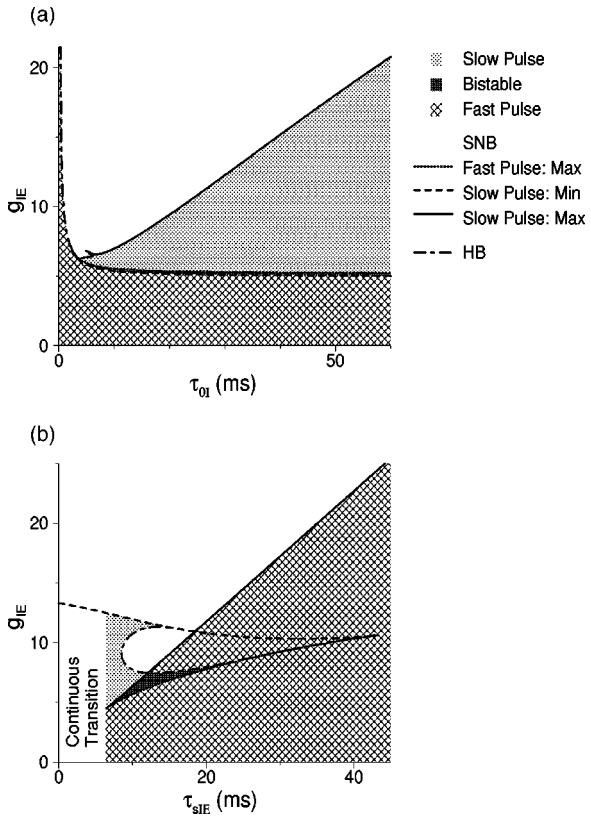

FIG. 10. (a) Regimes of existence and stability of fast and/or slow pulses in the τ_{0I}-g_{IE} plane (a) and in the τ_{sIE}-g_{IE} plane (b). In (b), $\tau_{sII}=\tau_{sIE}$. The meanings of the lines and the shading are the same as in Fig. 5. Slow pulses can propagate in a wider parameter regime if the passive time constant of inhibitory cells is large, whereas fast pulses can propagate in a wider parameter regime if inhibition decays slowly with time.

E. Effects of footprint lengths

For the reference parameter set, we use the values $\sigma_{EE}=\sigma_{EI}=1$, $\sigma_{IE}=\sigma_{II}=0.5$. The rationale behind this choice of parameters is that excitatory pyramidal cells in general, and especially the pyramidal neurons of layer V in neocortex, have a more horizontally widespread axonal arborization in comparison with the inhibitory neocortical neurons [18]. Except for this qualitative information, the relationships between the four footprint lengths $\sigma_{\beta\alpha}$ are not known. In some numerical simulations of conductance-based models of excitatory and inhibitory neurons [19], propagating pulses were obtained for $\sigma_{IE}>\sigma_{EE}$. We, therefore, consider the effects of varying the footprint lengths. In Fig. 11(a), we vary σ_{IE} and σ_{II} while keeping the equality $\sigma_{IE}=\sigma_{II}$, for $g_{IE}=6$. As σ_{IE} and σ_{II} increase, ν increases and ζ increases from a negative value of a few tens of ms to a negative value of a few ms. This implies that for this specific value of g_{IE}, increasing the inhibitory footprint lengths causes the pulse properties to evolve gradually from those of a ''slow'' pulse to those of a ''fast'' pulse. To further explore effects of varying the inhibitory footprint lengths at various g_{IE} values, we

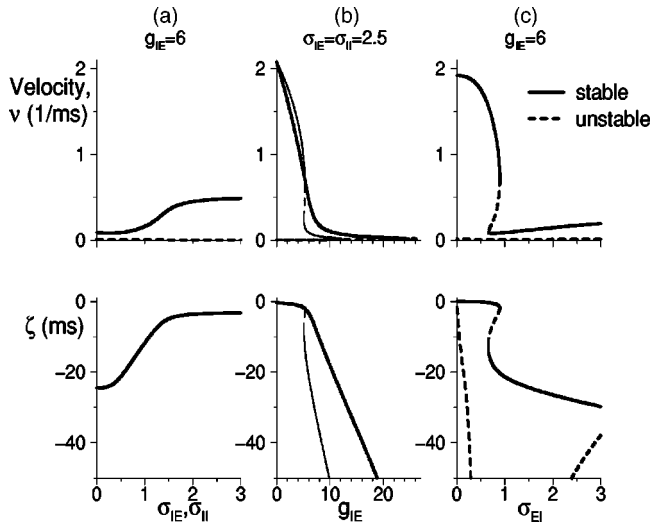

FIG. 11. Effects of varying the spatial coupling decay lengths. The velocity ν (upper panels) and the time difference ζ (lower panels) of propagating pulses are plotted as function of three parameters. Solid lines represent stable pulses and dashed lines represent unstable pulses. (a) The connectivity lengths σ_{IE} and σ_{II} are varied for $\sigma_{II}=\sigma_{IE}$ and $g_{IE}=6$. (b) The conductance g_{IE} is varied for $\sigma_{II}=\sigma_{IE}=2.5$ (thick lines) and $\sigma_{II}=\sigma_{IE}=0.5$ [thin lines, identical to the thick lines in Fig. 3(b)]. (c) The connectivity length σ_{EI} is varied.

show the values of ν and ζ as a function of g_{IE} in Fig. 11(b) for two values of σ_{IE} and σ_{II}: 2.5 (thick lines) and 0.5 (thin lines). For both cases, there is a transition, from a fast pulse at low g_{IE} to a slow pulse at high g_{IE}. The transition is more gradual for larger σ_{IE} and σ_{II}, and occurs at higher values of g_{IE}. These results show that the two types of pulses can be obtained both in cases where inhibition is less widespread than excitation and in cases where inhibition is more widespread than excitation.

As the E-to-I footprint length σ_{EI} increases, the pulse form switches from a fast pulse to a slow pulse, as shown in Fig. 11(c). This result can be explained by the fact that when the slow pulse propagates, I cells fire much before the E cells. If σ_{EI} is more widespread than σ_{EE}, I cells receive excitatory inputs before their neighboring E cells, and therefore have higher chances to fire before these E cells, and to slow down the pulse.

F. I-to-I conductance prevents the slow pulse and may cause irregular pulse propagation

The I-to-I conductance g_{II} was found to strongly affect the firing properties of networks under steady-state conditions [20,21]. In order to examine how g_{II} affects pulse propagation, we study the regimes where various types of pulses can propagate in a two-parameter, g_{II}-g_{IE} plane, as shown in Fig. 12(a). In this figure, solid and dotted lines represent saddle-node bifurcation in which slow and fast pulses are terminated, respectively, as g_{IE} values are increased. In addition, pulses with large enough g_{II} are terminated because the solution violates Eq. (9). Specifically,

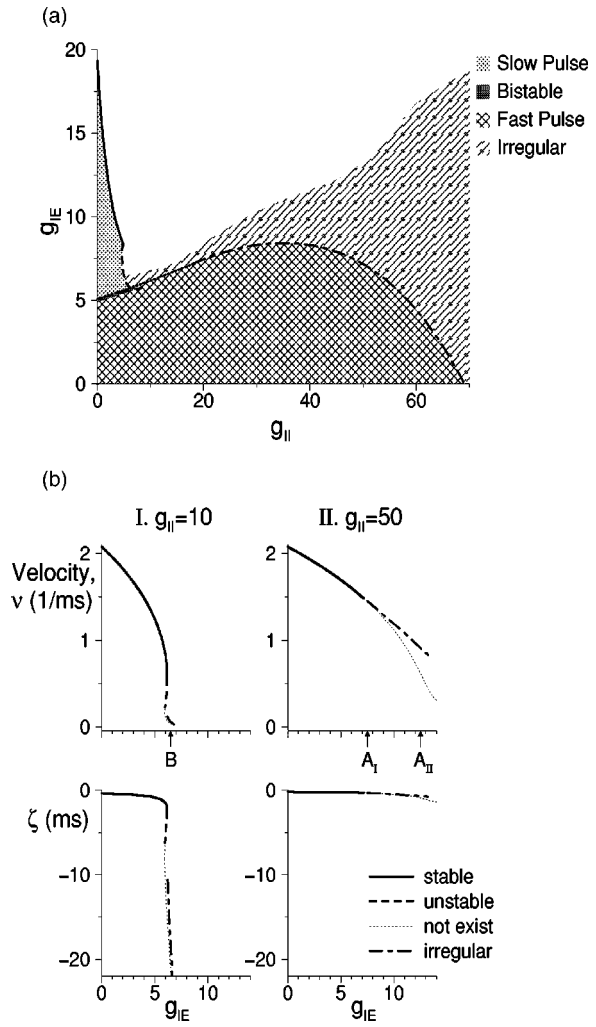

FIG. 12. (a) Regimes of existence and stability of fast and/or slow pulses in the g_{II}-g_{IE} plane. Saddle-node bifurcation lines: solid line, termination of the slow pulse; dotted line, termination of the fast pulse. Terminations of solutions because of Eq. (9): dashed line, slow pulse; dot-dashed line, fast pulse. Shadings: dark gray, bistable regime; light gray, regime in which only slow pulses can propagate; mesh of diagonal lines, regime in which only fast pulses can propagate; bent diagonal lines, irregular pulses. (b) The velocity ν (upper panels) and the time difference ζ (lower panels) of propagating pulses as functions of g_{IE} for $g_{II}=10$ (I) and $g_{II}=50$ (II). Line types: thick solid lines, stable traveling pulses; thick dashed lines, unstable pulses; thin dotted lines, (unphysical) values for ν and ζ that are obtained by solving Eqs. (14),(15); dot-dashed lines, irregular pulses, computed using numerical simulations. The arrows below the abscissa of the upper panels correspond to the g_{IE} values of Fig. 13. Strong inhibitory-to-inhibitory conductance eliminates the slow pulses and converts the fast traveling pulses into irregular pulses.

$$\frac{dV_I[-\zeta\nu, T_I(-\zeta\nu)]}{dt} > 0. \tag{36}$$

Such a termination is denoted by a dashed line for the slow pulse and by a dot-dashed line for the fast pulse. The bistable regime and the regimes in which either slow or fast pulses

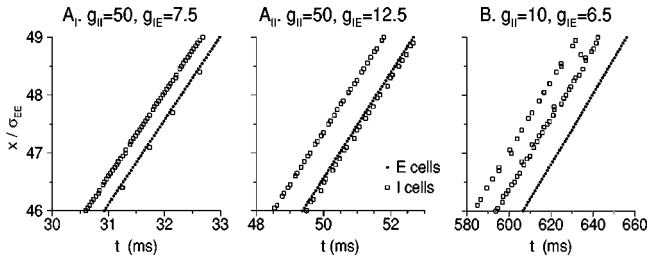

FIG. 13. Examples of neuronal firing times during the propagation of irregular pulses is shown for the reference parameter set and: A_I: $g_{II}=50$, $g_{IE}=7.5$, $\nu=1.45$ ms^{-1}; A_{II}: $g_{II}=50$, $g_{IE}=12.5$, $\nu=0.91$ ms^{-1}; B: $g_{II}=10$, $g_{IE}=6.5$, $\nu=0.06$ ms. Firing times of excitatory cells are denoted by solid circles, and firing times of inhibitory cells are denoted by open squares. There are $\rho=20$ neurons from each type within each unit length (σ_{EE}), and spikes of all the neurons are plotted. The number of neurons in each population is $N=1000$ and the total length of the system is $50\sigma_{EE}$.

can propagate are shaded as in the other two-parameter figures. The slow pulse can propagate only if g_{II} is small enough, and its regime of existence shrinks rapidly as g_{II} increases. At low g_{II} value, the slow pulse is terminated as g_{IE} increases by a SNB, and at higher values, it is terminated because of Eq. (36). Fast pulses are terminated by SNB (as g_{IE} increases) for much larger g_{II} values in comparison with the slow pulses. At even larger g_{II} values, however, these pulses are terminated by the condition of Eq. (36). The dependence of ν and ζ on g_{IE} for two values of g_{II}, 10 and 50, is shown in Fig. 12(b). For $g_{II}=10$, the fast traveling pulse is terminated by a SNB, whereas for $g_{II}=50$, it is terminated by condition (36).

What happens beyond the curve on which a pulse is terminated by condition (36)? Surprisingly, we find in numerical simulations that irregular pulses can propagate. Three examples of such pulses are shown in the rastergrams of Fig. 13. These pulses are characterized by the fact that excitatory cells fire almost as in regular traveling pulses, whereas inhibitory cells segregate into two spatiotemporal clusters. Neurons in the first cluster fire before their excitatory neighbors almost with a constant time delay $|\zeta_1|$. Neurons in the second cluster fire after their inhibitory neighbors from the first clusters, and often [as in Fig. 13(A), $g_{II}=50$] also after their neighboring excitatory neurons. The pulses in Fig. 13(A) have the characteristics of a fast pulse: inhibitory cells fire either less than 1 ms before neighboring excitatory cells or just after them, and ν is large [1.45 ms^{-1} in (I) and 0.91 -1/ms in (II)]. In Fig. 13(B) ($g_{II}=10$), all the inhibitory neurons fire before the neighboring excitatory neurons, and the segregation into two clusters is less strict. The pulse in Fig. 13(B) has characteristics of a slow pulse: inhibitory cells fire tens of ms before their neighboring excitatory cells, and ν is small (0.06 ms^{-1}).

In order to define the border of the appearance of the irregular pulses, we carried out numerical simulations in which we started from shock initial conditions and found out whether a pulse can propagate. The results are shown in the regime shaded by the bent diagonal lines in Fig. 12(a). We cannot rule out the possibility that pulses that are excited by different initial conditions propagate also outside of this regime. In Fig. 12(b), we compared the velocity ν and the average delay ζ of the irregular pulses (dot-dashed line) to the values of ν and ζ of the ''nonexisting pulses''—the solution of Eqs. (14),(15) that violates condition (36). The average value of $|\zeta|$ of the irregular pulses is smaller than $|\zeta|$ of the ''nonexisting pulse,'' and, as a result, ν is larger.

We can understand the appearance of irregular pulses by using the following argument. The strong mutual inhibition between inhibitory neurons at large g_{II} values prevents the propagation of a regular traveling pulse because when one I cell fires, it reduces the propensity of its neighboring I cell to fire afterward. As a result, neighboring I cells tend to fire with time delays between them.

V. FINITE AXONAL CONDUCTANCE VELOCITY

A. Traveling pulse solution with finite axonal conductance velocity

The response of a postsynaptic neuron to a firing of a presynaptic cell is delayed because the conductance velocity of action potential in axons is a finite value, denoted here by c. For finite c, the Volterra equations for the firing times $T_\alpha(x)$ become

$$V_{T\alpha}=\sum_{\gamma=f,s} g_{E\alpha}^{\gamma}\int_{-\infty}^{\infty}dx' w_{E\alpha}(x')G_{E\alpha}^{\gamma}\left[T_\alpha(x) - T_E(x-x')-\frac{|x'|}{c}\right]-g_{I\alpha}\int_{-\infty}^{\infty}dx' w_{I\alpha}(x') \times G_{I\alpha}\left[T_\alpha(x)-T_I(x-x')-\frac{|x'|}{c}\right]. \tag{37}$$

Assuming a traveling pulse solution, Eq. (11), and defining

$$\nu_-=\left(\frac{1}{\nu}-\frac{1}{c}\right)^{-1}, \quad \nu_+=\left(\frac{1}{\nu}+\frac{1}{c}\right)^{-1}, \tag{38}$$

one obtains for $\zeta<0$,

$$V_{TE}=\sum_{\gamma=f,s} g_{EE}^{\gamma}\int_0^{\infty}dx w_{EE}(x)G_{EE}^{\gamma}\left(\frac{x}{\nu_-}\right) - g_{IE}\int_{-\zeta\nu_-}^{\infty}dx w_{IE}(x+\zeta\nu_-)G_{IE}\left(\frac{x}{\nu_-}\right) - g_{IE}\int_0^{-\zeta\nu_-}dx\frac{\nu_+}{\nu_-}w_{IE}\left[\frac{\nu_+}{\nu_-}(x+\zeta\nu_-)\right]G_{IE}\left(\frac{x}{\nu_-}\right), \tag{39}$$

$$V_{TI}=\sum_{\gamma=f,s} g_{EI}^{\gamma}\int_0^{\infty}dx w_{EI}(x-\zeta\nu_-)G_{EI}^{\gamma}\left(\frac{x}{\nu_-}\right) - g_{II}\int_0^{\infty}dx w_{II}(x)G_{IE}\left(\frac{x}{\nu_-}\right). \tag{40}$$

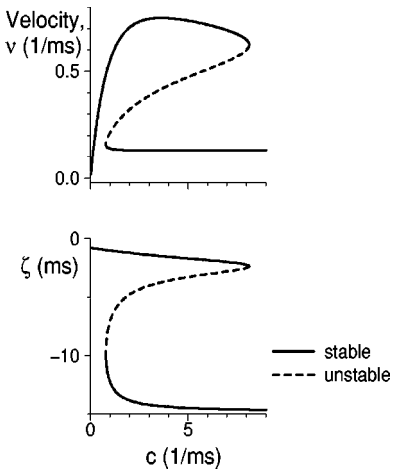

FIG. 14. The velocity ν of propagating pulses (upper panel), and the difference ζ between the firing times of inhibitory and excitatory cells at the same position (lower panel), as functions of the axonal conductance velocity c for the reference parameter and $g_{IE}=5.4$. The velocity of the fast pulse decreases with c near the SNB.

All the terms in Eqs. (39),(40), except for the ''backward'' term [the third integral in Eq. (39), representing the effect of the I cell spike on E cells with smaller x], are similar to the corresponding terms in Eqs. (12),(13), but the velocity ν there is replaced by ν_-. Using Eq. (5), one can see that in that ''backward'' term, there is an additional modification: σ_{IE} is replaced by $\sigma_{IE}\times\nu_-/\nu_+$. Since $\nu_->\nu_+$, this means that the length constant σ_{IE} is ''stretched'' in this term. Similar results are obtained for the EI term in the equations for $\zeta>0$.

In networks with excitation only, introducing finite axonal conductance velocity c reduces ν, because the term ν_- replaces ν in the dynamical equation [10]. In networks with excitation and inhibition, however, the factor ν_+ can play a role as well, and in principle, decreasing c may *increase* ν, as shown below.

B. Pulse velocity may decrease with c

Conduction velocity of unmyelined axons is of order 1 m/s [22,23]. Taking it into account is expected to affect mostly the fast pulses, whereas its effect on the slow pulses is expected to be very small. Indeed, numerical solutions of Eqs. (39),(40) show that in most cases, the velocity of the fast pulses is reduced if c is considered to be finite rather than infinite. There is, however, an exception that is shown in Fig. 14: the fast pulse exists at small c values but ceases to exists at a SNB at a critical c values. For a range of c values smaller than this critical value, the pulse velocity decreases with c. For this particular parameter regime, a slow pulse can also propagate if c is not too small, and its velocity is almost independent of c.

The decreasing ν with increasing c may occur in parameter regimes in which the fast pulse does not exist for $c\to\infty$, but exists if c is smaller than a certain value of a SNB. At a SNB, a stable branch and an unstable branch of solutions should coalesce and eliminate each other. In order to enable this coalescence, the upper, stable branch should ''bend'' toward the lower, unstable branch, and as a result ν should decrease at c values lower than the SNB values. This intuitively unexpected result demonstrates the nonlinear dynamics nature of the pulse propagation phenomenon.

VI. DISCUSSION

A. Properties of fast and slow pulses

Analysis of models of interacting excitatory and inhibitory neuronal populations with spatially decaying connectivity reveals that two types of pulses can propagate. Fast pulses can be regarded as a continuation of propagating pulse states in networks with only excitatory populations. They are characterized by E cells firing before or just after the neighboring I cells, and by monotonic increase of the neuronal potential before the firing. Slow pulses are characterized by E cells firing substantially after the I cells, and by a decrease in the potential of the E cells before a subsequent potential increase until the neuron reaches threshold and fires. As a parameter of the system varies, the transition from a fast-pulse parameter regime to a slow-pulse parameter regime can occur through a bistable regime, in which both types of pulses can propagate. It can also occur continuously, as the velocity of the pulses decreases and the time lead of I cell firing in comparison with E cell firing increases. A third possibility is that the fast pulse stops propagating as a parameter is varied, and a slow pulse appears in a distant parameter regime. The existence of propagating fast and slow pulses with the possibility of bistability was reported in Ref. [12]. In this article, we pursue our investigation of the properties of these two pulse types and their dependence on network parameters, as summarized here.

Fast pulses are robust with respect to initial conditions. If they are stable, a strong enough initial shock will evoke them. In contrast, slow pulses are not so robust. Even if they are stable, an initial shock often does not evoke them. Even if it does, the system dynamics can converge into this state after a long transient with fast or lurching pulse characterization.

Slow pulses can propagate even without slow excitation, but the parameter regime in which they are stable strongly expands as the level of slow E-to-E excitatory conductance g^s_{EE} increases. Moreover, slow excitation increases the basin of attraction of slow pulses and the possibility of evoking them with shock initial conditions. Fast pulses are hardly affected by slow excitation, as was shown in models of networks of excitatory neurons [6]. The parameter regime in which fast pulse can propagate, as well as their velocity, strongly increase as the level of fast E-to-E excitatory conductance g^f_{EE} increases. In particular, the curve of maximal g_{IE} and g^f_{EI} for which fast pulses can propagate are convex as a function of g^f_{EE}. The dependence of the parameter regime in which slow pulse can propagate on g^f_{EE} is more complicated. There are conditions in which increasing g^f_{EE} supports the propagation of slow pulse, whereas in other conditions it prevents propagation.

The two pulse types behave differently with respect to changes in the kinetics of inhibitory cells and synapses. Increasing the passive time constant of inhibitory cells τ_{0I} decreases the regime in which fast pulses can propagate (although only slightly for moderate and large τ_{0I} values), but increases the regime of slow-pulse propagation. Increasing the decay time of inhibitory conductance increases the parameter regime in which fast pulses can propagate, and decreases, and even eliminates, the regime of slow-pulse propagation.

Increasing the inhibitory footprint (connectivity) ranges σ_{IE} and σ_{II} makes the transition from fast to slow pulse smoother, but does not seem to modify the qualitative properties of the behavior. In particular, I cells lead in firing (ζ is negative) during the slow pulse even if σ_{IE} and σ_{II} are large. Extending the E-to-I footprint range σ_{EI} tends to transfer the system from a fast-pulse state to a slow-pulse state, because the wider E-to-I connectivity causes I cells to receive their inputs before the E cells and fire earlier.

Enhancing the I-to-I conductance g_{II} decreases, then eliminates, the regime in which slow pulse can propagate. At high g_{II} values, even fast traveling pulse cannot propagate because of the ''repulsive'' interaction between inhibitory interneurons. Instead, the network exhibits irregular pulses, during which E cells fire almost as they fire during a regular traveling pulse, and I cell segregate into two groups, which fire with two different delay times with respect to their neighboring excitatory cells. Irregular pulses can be regarded as pulses with ''spatiotemporal clustering'' of inhibitory cells. These pulses are different than lurching pulses that are observed in excitatory networks with delay [10] or in networks of excitatory and inhibitory neurons with large, slow E-to-E excitation and all the other synapses decaying fast [12]. Lurching pulses are characterized by periods of activity propagation followed by periods of silence and no propagation. During irregular pulses activity does not stop, and there are no silent periods. The irregular pulses have spatiotemporal periodicity, at least approximately. From this respect, they are similar to lurching pulses.

B. Effects of approximations

The model described here is based on two approximations. First, the subthreshold neuronal dynamics is described by an integrate-and-fire model. Second, each neuron is allowed to fire only one spike. The first approximation does not seem to affect the main results of this paper, because the key response to the activity of neuron to propagating pulses is that it integrates the response of other excitatory and inhibitory neurons and fires if the time-integrated amount of excitation is strong enough. To further support this claim, we replaced the integrate-and-fire scheme by the Morris-Lecar model, a version of a conductance-based model [24], and find regimes of fast and slow pulses with bistability between them (not shown).

The one-spike approximation is exact in the limit of very prolonged refractory period or very strong synaptic depression. In the first case, a neuron cannot fire a second spike before the pulse has completely passed. In the second case, spikes other than the first one do not generate any postsynaptic effect. Far from these limits, however, this approximation can have an effect on the dynamical mechanisms of the slow-pulse propagation. In networks with excitatory populations only, the results of this model are qualitatively similar to the results obtained by simulations of conductance-based model (compare [8–10] with [6]). In two-population systems, however, other scenarios can happen. For example, in our model, the potential of excitatory neurons becomes negative (hyperpolarized) before it becomes positive again and the neuron can fire. If the I cells can fire several fast spikes, they can prevent the E cell from firing. The model described in this work can be regarded, therefore, as a paradigm for illuminating a possible mechanism for a slow-pulse propagation, which is the advanced firing of I cells. We have carried out preliminary simulations of conductance-based neuronal models, in which cells can fire many spikes, demonstrated a transition from a fast pulse to a slow pulse as g_{IE} increases. As in the one-spike model, inhibitory cells lead substantially in firing during the slow pulse, but not during the fast pulse, and slow E-to-E excitation was found to be important for propagation of slow, but not fast, pulses. Further analytical and numerical investigation of models with more spikes should be carried out to see whether there are alternative mechanisms for slow-pulse propagation in addition to the mechanism described here.

Even adjacent cortical neurons have a delay of about 2 ms [25,26]. The effects of this constant time delay on the propagation of pulses in excitatory-only network were addressed [10], and it was found that they substantially reduce the pulse velocity. The effects of constant delays on the propagation of slow pulses are smaller because these pulses are slow even without delay, and therefore they are neglected in this work for simplicity.

C. Dynamical system aspects

The existence and stability of the traveling pulse solution are studied using methods that resemble the existence and stability analysis of dynamical systems defined by sets of coupled ordinary differential equations (ODEs) [27]. In systems of coupled ODEs, stability analysis is carried out by assuming a small perturbation in the configuration (or phase) space and following its evolution in time. Here we assume a small perturbation in the firing time of a neuron at a certain position and follow its evolution in space. The Volterra representation of the pulse dynamics, Eq. (8), simplifies the stability analysis of the pulse. Using this formalism, we obtain an eigenvalue equation (27), and the pulse is stable if all its solutions have negative real parts. The stability analysis was therefore reduced to a regular bifurcation problem. There is, however, one difference between our system and systems of coupled ODEs, which is the ''causality'' criterion (9) that the pulse solutions should obey.

In several cases [e.g., Figs. 5 and 10(b)], we find numerically that a SNB line and a HB line intersect at a cusp bifurcation. As we noted previously, at the point of intersection, the linearization has a pair of conjugate imaginary eigenvalues *and* a zero eigenvalue. The local analysis of this bifurcation

(Gavrilov-Guckenheimer or fold-Hopf) is complicated (see Ref. [17], pp. 330–348) and requires further study in this particular example.

D. Comparison with other systems and models

Slow pulses are not seen in neuronal networks with excitation only [6, 8–10, 28–33], because the mechanism of their generation requires leading inhibition. In particular, the transition from a fast pulse state to a slow pulse state, which may be accompanied by a bistable regime, is a unique property of our system. It has not been observed in models of spatially extended one-dimensional excitable systems with diffusive coupling [34–36].

This work is devoted to studying propagation of neuronal activity into a silent regime, as observed experimentally in cortical networks. Different spatiotemporal patterns are obtained when ''waves of phases'' propagate within an active region, as described in Ref. [37].

Propagation of fast and slow pulses was observed in simulations of conductance-based models of networks of excitatory and inhibitory populations, provided that the inhibition has a more widespread connectivity than excitation [19]. The mechanisms responsible for the generation and propagation of the various pulses in that system still remains to be explored.

There have been population or firing rate models of propagating waves in one and two populations. A piecewise linear system was analyzed in Ref. [38] and more recently a general two-population model was studied using singular perturbation [39]. In Ref. [40], transient propagation of waves was numerically simulated in a model for binocular rivalry. In both Refs. [39] and [38], only fast waves are described. Whether bistability can occur in these firing rate models is unknown.

E. Relations to experiments

Several results of the present model can be compared with data from experiments on cortical slices. First, our theoretical work shows that slow pulses can propagate even without slow excitation, but slow excitation substantially enhances the parameter regime in which slow pulse can propagate. Experiments show that blocking the slow NMDA receptors blocked the slow pulse or greatly reduced its intensity [5], is consistent with the prediction. Second, our analysis shows that there can be an abrupt transition from a fast pulse to a slow pulse as inhibition is increased. Preliminary experimental results [11] confirm this prediction. Third, the proposed mechanism for slow-pulse propagation demands that inhibitory cells fire before their neighboring excitatory cells. This prediction can be tested by dual intracellular recording from adjacent excitatory and inhibitory neurons. Fourth, according to the theory, during the slow-pulse propagation, excitatory cells should be hyperpolarized by inhibitory cells before their potential increases again and they can fire. This theoretical result can be tested experimentally using intracellular recording. Note, however, that the shunting (and not hyperpolarizing) nature of certain types of inhibitory synapses may modulate this behavior. Fifth, if the total fast E-to-E synaptic conductance g_{EE}^{f} is substantially increased, for example, during certain types of learning tasks [15], the I-to-E inhibition and the E-to-I excitation should increase considerably in order to prevent the propagation of fast, epilepticlike pulses. This prediction can be tested by dual intracellular recording between neurons from the excitatory and inhibitory populations, and comparing the results with or without learning. Sixth, strong, and even moderate values of I-to-I inhibition prevent the propagation of the slow pulse. On the other hand, strong I-to-I inhibition seems to be necessary for generating stable states of persistent activity [20,21]. In experiments, the slow pulse is sometimes accompanied by a prolonged state of persistent activity [5]. Theoretical and experimental investigation of such systems should be carried out in order to examine how slow pulses and persistent activity can occur in the same system.

ACKNOWLEDGMENTS

We are thankful to E. Barkai, D. Hansel, P. Latham, J. Rubin, D. Saar, C. van Vreeswijk, and J.-Y. Wu for helpful discussions. This research was supported by Grant No. 9800015 from the United States–Israel Binational Science Foundation (BSF), Jerusalem, Israel, to D.G. and G.B.E.; it was supported in part by the National Science Foundation under Grant No. PHY99-07949 to G.B.E. D.G. thanks the Institute of Theoretical Physics, UCSB, where part of this work was carried out, for its hospitality.

APPENDIX A: ELEMENTS OF THE STABILITY MATRIX

Substituting Eqs. (5),(6) in Eqs. (23)–(26,) we obtain for $\zeta<0$,

$$A_{EE}(\lambda) = \sum_{\gamma} \frac{1}{2} g_{EE}^{\gamma} \tau_{0E} \nu^2 \left\{ \frac{1}{(\sigma_{EE}+\nu\tau_{0E})(\sigma_{EE}+\nu\tau_{sEE}^{\gamma})} - \frac{1+\lambda\sigma_{EE}}{[\sigma_{EE}+\nu\tau_{0E}(1+\lambda\sigma_{EE})][\sigma_{EE}+\nu\tau_{sEE}^{\gamma}(1+\lambda\sigma_{EE})]} \right\} - A_{IE}(0), \tag{A1}$$

$$A_{IE}(\lambda) = \frac{g_{IE}\tau_{0E}\nu}{2(\tau_{0E}-\tau_{sIE})} \left\{ \exp\left(\frac{\zeta}{\tau_{2I}}+\lambda\nu\zeta\right) \times \left[\frac{1}{\sigma_{IE}+\nu\tau_{sIE}(1+\lambda\sigma_{IE})} - \frac{1}{\sigma_{IE}-\nu\tau_{sIE}(1-\lambda\sigma_{IE})} \right] - \exp\left(\frac{\zeta}{\tau_{0E}}+\lambda\nu\zeta\right) \times \left[\frac{1}{\sigma_{IE}+\nu\tau_{0E}(1+\lambda\sigma_{IE})} - \frac{1}{\sigma_{IE}-\nu\tau_{0E}(1-\lambda\sigma_{IE})} \right] + \exp\left(\frac{\zeta\nu}{\sigma_{IE}}\right) \left[\frac{1}{\sigma_{IE}-\nu\tau_{sIE}(1-\lambda\sigma_{IE})} \right.$$

$$-\frac{1}{\sigma_{IE}-\nu\tau_{0E}(1-\lambda\sigma_{IE})}\Bigg]\Bigg\}, \tag{A2}$$

$$A_{EI}(\lambda)=-\sum_{\gamma}\frac{1}{2}g_{EI}^{\gamma}\tau_{0I}\nu^{2}\exp\left(\frac{\zeta\nu}{\sigma_{EI}}\right)\times\frac{1+\lambda\sigma_{EI}}{[\sigma_{EI}+\nu\tau_{0I}(1+\lambda\sigma_{EI})][\sigma_{EI}+\nu\tau_{sEI}^{\gamma}(1+\lambda\sigma_{EI})]}, \tag{A3}$$

$$A_{II}(\lambda)=-A_{EI}(0)-\frac{1}{2}g_{II}\tau_{0I}\nu^{2}\left\{\frac{1}{(\sigma_{II}+\nu\tau_{0I})(\sigma_{II}+\nu\tau_{sII})}-\frac{1+\lambda\sigma_{II}}{[\sigma_{II}+\nu\tau_{0I}(1+\lambda\sigma_{II})][\sigma_{II}+\nu\tau_{sII}(1+\lambda\sigma_{II})]}\right\}. \tag{A4}$$

Similar equations are obtained for $\zeta>0$.

APPENDIX B: $V_{\alpha}(X,0)$

For $\zeta<0$, Eq. (35) becomes

$$V_{E}(x,0)=\sum_{\gamma=f,s}C_{EE}^{\gamma}-C_{IE}, \tag{B1}$$

$$V_{I}(x,0)=\sum_{\gamma=f,s}C_{EI}^{\gamma}-C_{II}, \tag{B2}$$

where

$$C_{EE}^{\gamma}=g_{EE}^{\gamma}\frac{\tau_{0E}\sigma_{EE}\nu}{2(\nu\tau_{0E}+\sigma_{EE})(\nu\tau_{sEE}^{\gamma}+\sigma_{EE})}\exp\left(\frac{-x}{\sigma_{EE}}\right). \tag{B3}$$

For $x>-\zeta\nu$,

$$C_{IE}=g_{IE}\frac{\tau_{0E}\sigma_{IE}\nu}{2(\nu\tau_{0E}+\sigma_{IE})(\nu\tau_{sIE}+\sigma_{IE})}\exp\left(\frac{-x-\zeta\nu}{\sigma_{IE}}\right). \tag{B4}$$

For $0<x<-\zeta\nu$,

$$C_{IE}=g_{IE}\frac{\tau_{0E}\nu}{(\tau_{0E}-\tau_{sIE})}\left[\frac{\nu\tau_{sIE}^{2}}{\sigma_{IE}^{2}-\nu^{2}\tau_{sIE}^{2}}\exp\left(\frac{x+\zeta\nu}{\tau_{sIE}\nu}\right)-\frac{\nu\tau_{0E}^{2}}{\sigma_{IE}^{2}-\nu^{2}\tau_{0E}^{2}}\exp\left(\frac{x+\zeta\nu}{\tau_{0E}\nu}\right)+\frac{\sigma_{IE}(\tau_{0E}-\tau_{sIE})}{2(\sigma_{IE}-\nu\tau_{0E})(\sigma_{IE}-\nu\tau_{sIE})}\exp\left(\frac{x+\zeta\nu}{\sigma_{IE}}\right)\right], \tag{B5}$$

$$C_{EI}^{\gamma}=g_{EI}^{\gamma}\frac{\tau_{0I}\sigma_{EI}\nu}{2(\nu\tau_{0I}+\sigma_{EI})(\nu\tau_{sEI}^{\gamma}+\sigma_{EI})}\exp\left(\frac{-x}{\sigma_{EI}}\right), \tag{B6}$$

$$C_{II}=g_{II}\frac{\tau_{0I}\sigma_{II}\nu}{2(\nu\tau_{0I}+\sigma_{II})(\nu\tau_{sII}+\sigma_{II})}\exp\left(\frac{-x-\zeta\nu}{\sigma_{II}}\right). \tag{B7}$$

APPENDIX C: NUMERICAL TECHNIQUES

For solving Eqs. (14),(15), we extract ζ from Eq. (15). After substituting the term for ζ in Eq. (14), we obtain a single algebraic equation for ν, which we solve numerically in the interval of ν values for which ζ is guaranteed to be negative. Similarly, we extract ζ from Eq. (16), substitute it in Eq. (17), and solve the resulting equation in the regime in which ζ is guaranteed to be positive.

For calculating stability, we follow the solutions of Eqs. (27),(28) using XPPAUT [41]. This calculation is carried out separately for $\zeta<0$ and for $\zeta>0$.

[1] Y. Chagnac-Amitai and B.W. Connors, J. Neurophysiol. **61**, 747 (1989); **62**, 1149 (1989).

[2] N. Laaris, G.C. Carlson, and A. Keller, J. Neurosci. **20**, 1529 (2000).

[3] J.-Y. Wu, L. Guan, and Y. Tsau, J. Neurosci. **19**, 5005 (1999).

[4] J.-Y. Wu and L. Guan, J. Neurophysiol. **86**, 2416 (2001).

[5] M.V. Sanchez-Vives and D.A. McCormick, Nat. Neurosci. **3**, 1027 (2000).

[6] D. Golomb and Y. Amitai, J. Neurophysiol. **78**, 1199 (1997).

[7] D. Golomb, J. Neurophysiol. **79**, 1 (1998).

[8] G.B. Ermentrout, J. Comput. Neurosci. **5**, 191 (1998).

[9] P.C. Bressloff, Phys. Rev. Lett. **82**, 2979 (1999); J. Math. Biol. **40**, 169 (2000).

[10] D. Golomb and G.B. Ermentrout, Proc. Natl. Acad. Sci. U.S.A., **96**, 13480 (1999); Network **11**, 221 (2000).

[11] D. Golomb, G.B. Ermentrout, and J.-Y. Wu, Society for Neuroscience Abstracts **26**, 1467 (2000).

[12] D. Golomb and G.B. Ermentrout, Phys. Rev. Lett. **86**, 4179 (2001).

[13] H. Markram and M. Tsodyks, Nature (London) **382**, 807 (1996).

[14] F. C. Hoppensteadt and E. M. Izhikevich, *Weakly Connected Neural Networks* (Springer-Verlag, New-York, 1997).

[15] D. Saar, Y. Grossman, and E. Barkai, J. Neurosci. **19**, 8616 (1999).

[16] J.R. Gibson, M. Beierlein, and B.W. Connors, Nature (London) **402**, 75 (1999); M.R. Deans, J.R. Gibson, C. Sellitto, B.W. Connors, and D.L. Paul, Neuron **31**, 477 (2001).

[17] Y. A. Kuznetsov, *Elements of Applied Bifurcation Theory*, 2nd ed. (Springer, New York, 1998).

[18] C.D. Gilbert, Annu. Rev. Neurosci. **6**, 217 (1983).

[19] A. Compte, M.V. Sanchez-Vives, D.A. McCormick, and X.-J. Wang, Soc. Neurosci. Abstr. **26**, 1967 (2000).

[20] D. Golomb, D. Hansel, and G. Mato, in *Handbook of Biologi-*

cal Physics, Volume 4: Neuro-Informatics and Neural Modelling, edited by F. Moss and S. Gielen (Elsevier Science, New York, 2001), pp. 887–968.
[21] D. Hansel and G. Mato, Phys. Rev. Lett. **86**, 4175 (2001).
[22] L. B. Haberly, in *The Synaptic Organization of the Brain*, 3rd ed., edited by G. M. Shepherd (Oxford University Press, Oxford, 1990), pp. 317–345.
[23] Z. Gil and Y. Amitai, J. Neurosci. **16**, 6567 (1996).
[24] J. Rinzel and G. B. Ermentrout, in *Methods in Neuronal Modeling: From Ions to Networks*, 2nd ed., edited by C. Koch and I. Segev (MIT Press, Cambridge, MA, 1998), pp. 251–291.
[25] A.M. Thomson, J. Deuchars, and D.C. West, J. Neurophysiol. **70**, 2345 (1993).
[26] H. Markram, J. Lubke, M. Frotscher, A. Roth, and B. Sakmann, J. Physiol. (London) **500**, 409 (1997).
[27] J. Guckenheimer and P. Holmes, *Nonlinear Oscillations, Dynamical Systems, and Bifurcation of Vector Fields* (Springer, New York, 1983).
[28] R. D. Traub and R. Miles, *Neuronal Networks of the Hippocampus* (Cambridge University Press, New York, 1991); R.D. Traub, J.G.R. Jefferys, and R. Miles, J. Physiol. (London) **472**, 267 (1993).
[29] P.C. Bush, P.A. Prince, and K.D. Miller, J. Neurophysiol. **82**, 1748 (1999).
[30] W.M. Kistler, R. Seitz, and J.L. van Hemmen, Physica (Amsterdam) **114D**, 273 (1998).
[31] D. Horn and I. Opher, Philos. Mag. B **77**, 1575 (1998).
[32] C. Fohlmeister, W. Gerstner, R. Ritz, and J.L. van Hemmen, Neural Comput. **7**, 905 (1995).
[33] Pulses with very slow velocities may exist in networks with excitation only but they are unstable.
[34] M.C. Cross and P.C. Hohenberg, Rev. Mod. Phys. **65**, 851 (1993).
[35] J. P. Keener and J. Sneyd, *Mathematical Physiology* (Springer-Verlag, New York, 1998).
[36] E. Meron, Phys. Rep. **218**, 1 (1992).
[37] G.B. Ermentrout and D. Kleinfeld, Neuron **29**, 33 (2001).
[38] S.-I. Amari, Biol. Cybern. **27**, 77 (1977).
[39] D.J. Pinto and G.B. Ermentrout, SIAM (Soc. Ind. Appl. Math.) J. Appl. Math. **62**, 206 (2001).
[40] H.R. Wilson, R. Blake, and S.-H. Lee, Nature (London) **412**, 907 (2001).
[41] G. B. Ermentrout, XPPAUT 5.4, http://www.pitt. edu/~phase